Reversible Charge Separation Followed by Exciplex Formation

M. V. Petrova

International Tomography Center, Novosibirsk 630090, Russia, Novosibirsk State University, Novosibirsk, 630090, Russia

A. I. Burshtein*

Department of Chemical Physics, Weizmann Institute of Science 76100, Rehovot, Israel

Received: October 11, 2008; Revised Manuscript Received: December 13, 2008

The quenching of fluorescence by reversible bimolecular ionization, followed by reversible exciplex formation from an ion pair (Scheme II) subjected to spin-conversion and subsequent radical−ion recombination/separation, has been studied by means of integral encounter theory (IET) and fitted to the available experimental data. Using the incoherent (rate) model of spin-conversion, the ion recombination to the excited triplet products is also accounted for. All of the results are obtained and shown to be different for the pulse excitation of fluorescence and its stationary detection. The free-energy dependence of all of the calculated properties of the forward and backward electron transfer are specified and compared with the conventional free-energy gap (FEG) law.

I. Introduction

The creation of exciplexes from of counter-ions, A^- and D^+, created by distant electron transfer between light excited precursors, $A^* + D$ or $D^* + A$, is known as Scheme II of the exciplex formation proposed by Weller.[1−3] It is an alternative to Scheme 1, which has been just studied by means of integral encounter theory (IET).[9] In the spinless theory, the reaction Scheme II can be presented as follows: where the forward

$$\begin{array}{ccccc} A + D & \underset{1/\tau_A}{\overset{I}{\rightleftharpoons}} & {}^1A^* + D & & \\ & & W_F \downarrow\uparrow W_B & & \\ [A^\delta\ D^{\delta+}] & \underset{k_a}{\overset{k_d}{\rightleftharpoons}} & {}^1[A^- \cdots D^+] & \rightleftharpoons & A\ + D^+ \\ \downarrow\ 1/\tau_e & & \downarrow W_R & & \\ [A\ D] & & A + D & & \end{array} \qquad (1.1)$$

(ionization) and backward electron transfer rates, $W_F(r)$ and $W_B(r)$, are space dependent, as well as that of recombination to the ground-state products, $W_R(r)$. The ions' association into an exciplex, as well as dissociation of the latter, are considered as contact reactions with corresponding rate constants:

$$k_a = k_d v \exp(-\Delta G_{RIP}/T) \qquad (1.2)$$

where ΔG_{RIP} is the free energy of exciplex formation from the radical ion pair (RIP), which is negative in Figure 1, and v is approximately the volume of attached reaction layer[10,11] (hereafter the Boltzmann constant $k_B = 1$). The exciplex formation is known to proceed in the narrow region around $\Delta G_i = 0$, where ΔG_i is the free energy of ionization.

The excited electron acceptor A^* and the exciplex $[A^{\delta-}D^{\delta+}]$ decay with the rates $1/\tau_A$ and

$$\frac{1}{\tau_e} = \frac{1}{\tau_A} \frac{1}{1 + (\Delta G_{exc}/V)^2} \qquad (1.3)$$

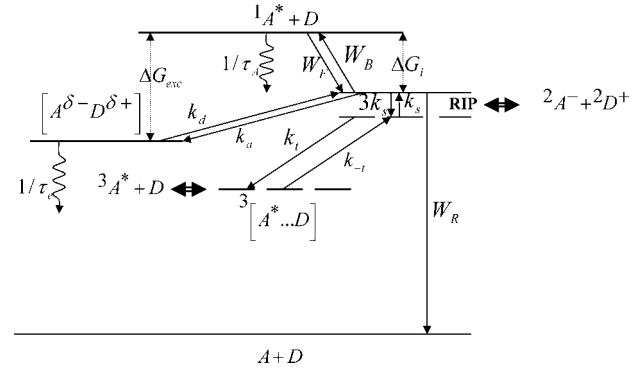

Figure 1. General reaction scheme of the reversible ionization and subsequent exciplex formation/dissociation accounting for the spin conversion in the radical−ion pair followed by their recombination and reversible triplet formation.

where

$$\Delta G_{exc} = \Delta G_i/2 - \sqrt{(\Delta G_i/2)^2 + V^2} = \Delta G_i + \Delta G_{RIP} \qquad (1.4)$$

Here, V is the electron coupling between A^*D and A^-D^+ and ΔG_i is the free energy of initial ionization (RIP formation). The fluorescence of the exciplex and the charge separation δ are weaker, the smaller is the mixing of the excited and ion pair states, due to electron tunneling.[4−7,9]

The light excitation may be either instantaneous, $I = N_0/N$ $\delta(t)$, or stationary, $I = I_0 = \text{const}$ (here, $N = [A]$ and $N^* = [A^*]$ at $t = 0$). We will consider first the quantum yields of fluorescence following pulse excitation and products of geminate RIP recombination/separation assisted by spin-conversion. Then the florescence quenching under permanent illumination will be investigated, as well as the stationary concentrations of the free ions and triplet excitations.

II. Pulse Excitation

A. Spin-Assisted Reaction. As a matter of fact, the RIP born in its singlet state is subjected to spin-conversion that makes

* Corresponding author.

10.1021/jp809015t CCC: $40.75
Published on Web 02/12/2009

possible the backward electron transfer to the triplet neutral product (Figure 1):

$$\begin{array}{ccccc} & & A^* + D & & \\ & & W_F \downarrow\uparrow W_B & & \\ [A^{\delta-}D^{\delta+}] & \underset{k_a}{\overset{k_d}{\rightleftharpoons}} & {}^1[A^- \cdots D^-] & \rightleftharpoons & {}^2A^- + {}^2D^+ \\ \downarrow\ 1/\tau_e & & k_s \uparrow\downarrow 3k_s & & \\ & & {}^3[A^- \cdots D^-] & \rightleftharpoons & {}^2A + {}^2D \\ & & k_{-t} \uparrow\downarrow k_t & & \\ & & {}^3[A^* \cdots D] & \rightleftharpoons & {}^3A^* + D \end{array} \qquad (2.1)$$

This reaction is parallel to the straightforward recombination of the singlet RIP to the ground state, with the rate $W(r)$ shown in Scheme 1.1. We are using here the simplest (incoherent) model of spin conversion proceeding with the rate k_s between the spin components. It was shown to be a good approximation for the coherent HFI-induced spin-conversion in zero magnetic fields.[12,13] The reversible production of an excited acceptor/donor pair occurs with the rate constant k_t, whereas the backward reaction has the rate k_{-t}, and they are related to each other as follows:

$$k_t = k_t^0 e^{-[(\Delta G_t+\lambda)^2]/4\lambda T} = k_{-t}\exp(-\Delta G_t/T) \qquad (2.2)$$

Here, the free energy of triplet creation is $\Delta G_t = E_T - E_S - \Delta G_i < 0$, where E_S and E_T are the excitation energy of singlet and triplet excitations $^1A^*$ and $^3A^*$.

B. IET of the Pulse-Induced Reaction. When the system response after δ-pulse excitation is traced in a limited time domain, the bulk reactions have no time to develop provided acceptor concentration is reasonably small. What follows excitation in such a case is actually the geminate reaction finishing with products separation. For Scheme II with parallel singlet and triplet recombination channels, it is described by the matrix IET developed in ref 14, allowing us to get the following set of linear equations for the state populations of excitations (N^*), exciplexes (N^e), RIPs (P), and triplets (N^T):

$$\frac{d}{dt}N^* = -c\int_0^t R_{11}(t-\tau)N^*(\tau)\,d\tau + \int_0^t R_{12}(t-\tau)N^e(\tau)\,d\tau - \frac{N^*}{\tau_A} + IN$$

$$\frac{d}{dt}N^e = c\int_0^t R_{21}(t-\tau)N^*(\tau)\,d\tau - \int_0^t R_{22}(t-\tau)N^e(\tau)\,d\tau - \frac{N^e}{\tau_e}$$

$$\frac{d}{dt}P = c\int_0^t R_{31}(t-\tau)N^*(\tau)\,d\tau + \int_0^t R_{32}(t-\tau)N^e(\tau)\,d\tau$$

$$\frac{d}{dt}N^T = c\int_0^t R_{41}(t-\tau)N^*(\tau)\,d\tau + \int_0^t R_{42}(t-\tau)N^e(\tau)\,d\tau$$

Here,

$$c = [D] \gg [A] = N;\quad N \gg [A^*] = N^*;\quad [A^-] = [D^+] = P;\quad N^e = [A^{\delta-}D^{\delta+}]$$

and $I(t)$ is the rate of the light pumping. If the latter is instantaneous, $I = N_0/N\ \delta(t)$, the term IN should be omitted and the resulting equations have to be solved with an initial condition: $N^*(0) = N_0$; $N^e = P = N^T = 0$. The measurable quantities are the kinetics of the excitations and exciplexes luminescence (at different frequencies) from what the yields of both can be obtained:

$$\eta = \frac{\int_0^\infty N^*(t')\,dt'}{N_0\tau_A} = \frac{\tilde{N}^*(0)}{N_0\tau_A} = \frac{1}{1 + c\tau_A\kappa_g} \qquad (2.3)$$

$$\eta^e = \frac{\int_0^\infty N^e(t')\,dt'}{N_0\tau_e} = \frac{\tilde{N}^e(0)}{N_0\tau_e} = (1-\eta)\varphi^e \qquad (2.4)$$

where the geminate Stern−Volmer constant is

$$\kappa_g = \tilde{R}_{11}(0) - \frac{\tilde{R}_{12}(0)\tilde{R}_{21}(0)}{\tilde{R}_{22}(0) + 1/\tau_e} \qquad (2.5)$$

and the exciplex fraction of RIP recombination is

$$\varphi^e = \frac{\tilde{R}_{21}(0)}{\tilde{R}_{11}(0) + \tau_e(\tilde{R}_{11}(0)\tilde{R}_{22}(0) - \tilde{R}_{12}(0)\tilde{R}_{21}(0))} \qquad (2.6)$$

The free ions and triplets have the yields

$$\phi = P(\infty)/N_0 = (1-\eta)\varphi \qquad (2.7)$$

$$\phi^T = N^T(\infty)/N_0 = (1-\eta)\varphi^T \qquad (2.8)$$

where the charge separation quantum yield is

$$\varphi = \frac{\tilde{R}_{31}(0) + \tau_e(\tilde{R}_{22}(0)\tilde{R}_{31}(0) + \tilde{R}_{21}(0)\tilde{R}_{32}(0))}{\tilde{R}_{11}(0) + \tau_e(\tilde{R}_{11}(0)\tilde{R}_{22}(0) - \tilde{R}_{12}(0)\tilde{R}_{21}(0))} \qquad (2.9)$$

and the triplet fraction of RIP recombination is

$$\varphi^T = \frac{\tilde{R}_{41}(0) + \tau_e(\tilde{R}_{22}(0)\tilde{R}_{41}(0) + \tilde{R}_{21}(0)\tilde{R}_{42}(0))}{\tilde{R}_{11}(0) + \tau_e(\tilde{R}_{11}(0)\tilde{R}_{22}(0) - \tilde{R}_{12}(0)\tilde{R}_{21}(0))} \qquad (2.10)$$

There is of course the conservation law:

$$\varphi^S = 1 - \varphi - \varphi^T - \varphi^e \qquad (2.11)$$

where φ^S is the fraction of ion pairs recombined into ground state.

C. Contact Approximation. The rate of the electron transfer proceeding in the normal Marcus region decreases in space quasi-exponentially and rather fast.[8] This function is often modeled by a $\delta(r-\sigma)$-function assuming that the reaction proceeds only at contact distance σ between the reacting particles. The contact approximation is very popular from the Smoluchowski times. In this approximation, the integral kernels $\tilde{R}_{ij}$ can be easily specified. They are expressed via the rate constants of contact reactions and auxiliary functions g_i, which account for the transient effects:

$$\tilde{R}_{11}(s) = \frac{k_F}{Y}[(4 + (k_a + k_c)(3g_3 + g_4))(1 + k_{-t}g_5) + (3g_4 + g_3 + 4g_3g_4(k_a + k_c))k_t] \qquad (2.12a)$$

$$\tilde{R}_{12}(s) = \frac{k_dk_B}{Y}[(3g_3 + g_4)(1 + k_{-t}g_5) + 4g_3g_4k_t] = \frac{k_ak_F}{k_dk_B}\tilde{R}_{21} \qquad (2.12b)$$

$$\tilde{R}_{22}(s) = \frac{k_d}{Y}[(1 + k_{-t}g_5)((1 + k_Fg_1)(4 + k_c(3g_3 + g_4)) + k_B(3g_3 + g_4)) + k_t((g_3 + 3g_4 + 4g_3g_4k_c)(1 + k_Fg_1) + 4g_3g_4k_B)] \qquad (2.12c)$$

$$\tilde{R}_{31}(s) = \frac{4k_F}{Y}(1 + g_5k_{-t} + g_3k_t) \qquad (2.12d)$$

$$\tilde{R}_{32}(s) = \frac{4k_d}{Y}(1 + k_F g_1)(1 + g_5 k_{-t} + g_3 k_t) \quad (2.12e)$$

$$\tilde{R}_{41}(s) = \frac{3k_F k_t}{Y}(g_4 - g_3) \quad (2.12f)$$

$$\tilde{R}_{42}(s) = \frac{3k_t k_d}{Y}(g_4 - g_3)(1 + k_F g_1) \quad (2.12g)$$

$$Y = (1 + k_{-t}g_5)[(1 + k_F g_1)(4 + (k_a + k_c)(3g_3 + g_4)) + k_B(3g_3 + g_4)] + k_t[(1 + k_F g_1)(4g_3 g_4(k_a + k_c) + g_3 + 3g_4) + 4k_B g_3 g_4] \quad (2.12h)$$

Here, the contact forward and backward electron transfer is represented by the corresponding rate constants

$$k_F = k_B e^{-\Delta G_i/T} = \int_\sigma^\infty W_F(r) 4\pi r^2 \, dr = k_F^0 e^{-[(\Delta G_I + \lambda)^2]/4\lambda T} \quad (2.13)$$

Similarly,

$$k_c = \int_\sigma^\infty W_R(r) 4\pi r^2 \, dr = k_c^0 e^{-[(\Delta G_r + \lambda)^2]/4\lambda T} \quad \text{where} \quad \Delta G_r = -E_S - \Delta G_i \quad (2.14)$$

The auxiliary functions are[9]

$$g_1(s) = \frac{1}{k_D}\frac{1}{1 + \sqrt{\tau_d\left(s + \frac{1}{\tau_A}\right)}}, \quad g_5(s) = \frac{1}{k_D}\frac{1}{1 + \sqrt{\tau_d s}} \quad (2.15)$$

where $\tau_d = \sigma^2/D$ is an encounter time in free space, whereas $k_D = 4\pi\sigma D$ is the diffusional rate constant in contact approximation. The rest of the g-functions

$$g_3(s) = \int u_3(t) e^{-st} \, dt \quad \text{and} \quad g_4(s) = \int u_4(t) e^{-st} \, dt \quad (2.16)$$

are the Laplace transformations of the Green Functions, $u_3(t)$ and $u_4(t)$, which obey the kinetic equations presented and solved in our previous article.[9]

D. Yields of Luminescence and RIP Decay products. Using all of this information, we obtain from section 2.5 the following expression for the geminate Stern−Volmer constant:

$$\frac{1}{\kappa_g} = \frac{1}{\kappa_i} + \frac{1}{K_{eq}(k_{esc} + k_c + k_{exc})} \quad \text{where} \quad K_{eq} = k_F/k_B = e^{-\Delta G_i/T} \quad (2.17)$$

and the rate constant of reversible exciplex formation is

$$k_{exc} = \frac{k_a}{1 + k_d\tau_e} = \begin{cases} k_a & \text{irreversible formation} \\ v e^{-\Delta G_{RIP}/T}/\tau_e & \text{reversible formation} \end{cases} \quad (2.18)$$

When ionization is exergonic ($\Delta G_i < 0$), the exciplex formation is reversible but its rate constant increases with $|\Delta G_{RIP}|$ reaching finally the upper limit k_a, corresponding to irreversible exciplex formation after endergonic ionization.

As for κ_i, this is the well-known irreversible analogue of κ_g that comes from it when $k_B = 0$ ($K_{eq} \to \infty$),

$$\frac{1}{\kappa_i} = \frac{1}{k_F} + \frac{1}{k_D(1 + \sqrt{\tau_d/\tau_A})} \quad (2.19)$$

whereas the rate constant of cage escape (charge separation) in highly polar solvents (Onsager radius $r_c \to 0$) is:[9]

$$k_{esc} = k_D\left[1 + \frac{3\sqrt{4k_s\tau_d}(k_D + k_t + k_{-t})}{(4(k_D + k_t + k_{-t}) + \sqrt{4k_s\tau_d}(k_D + k_{-t}))}\right] \quad (2.20)$$

In the absence of spin-conversion, $k_{esc} \equiv k_D$ and monotonously increases with k_s but in finite limits:

$$k_D < k_{esc} < 4k_D\left[1 + \frac{3}{4}\frac{k_t}{k_D + k_{-t}}\right] \quad (2.21)$$

If the RIP does not recombine to the triplet ($k_t = 0$), then the upper limit is only 4 times larger than the lower one because at fast equilibration ($k_s \to \infty$) all 4 states of the RIP are subjected to separation instead of the singlet one. The border between these limit $\sqrt{(4k_s\tau_d)} \approx 2$ establishes the criterium of spin-states equilibration: $k_s\tau_d \gg 1$. Anyhow, the triplet recombination channel adds just a little to the cage escape constant.

In contact approximation, the yield of exciplex production (from the RIP) defined in eq 2.6 takes in polar solvents the following form:

$$\varphi^e = \frac{k_{exc}}{k_c + k_{esc} + k_{exc}} \quad (2.22)$$

where k_{esc} is given by eq 2.20 and k_{exc} by eq 2.18.

The yield (eq 2.10) of contact triplet production in polar solvents takes the form:

$$\varphi^T = k_t\frac{k_{esc} - k_D}{[1 + (k_t/(k_D + k_{-t}))][k_c + k_{esc} + k_{exc}]} \quad (2.23)$$

In the absence of spin conversion ($k_s = 0$), there are no triplet RIPs and no triplet products: $\varphi^T = k_{esc} - k_D = 0$, but with growing k_s the triplet yield increases reaching its maximum value:

$$\varphi^T_{max} = \frac{3k_t}{k_D + k_{-t}}\frac{k_D}{k_c + k_D[4 + (3k_t/(k_D + k_{-t}))] + k_{exc}} \le \frac{3}{4}\frac{k_t}{k_D + k_{-t}} \quad (2.24)$$

The charge separation yield (eq 2.9) also saturates with k_s:

$$\varphi = \frac{4k_D}{[k_c + k_{esc} + k_{exc}]}\frac{(1 + \sqrt{4k_s\tau_d})(k_D + k_{-t}) + k_t}{(4 + \sqrt{4k_s\tau_d})(k_D + k_{-t}) + 4k_t} \quad (2.25)$$

In the spinless theory, we obtain from here:

$$\varphi = \frac{k_D}{k_c + k_D + k_{exc}} \quad \text{where} \quad k_s = 0 \quad (2.26)$$

If the formation of the exciplex is also impossible, this result reduces to the conventional formula of the exponential model in the zero Coulomb field:

$$\varphi = \frac{k_D}{k_c + k_D} = \frac{1}{1 + z/D} \quad \text{where} \quad k_s = k_{exc} = 0 \quad (2.27)$$

where

$$z = k_c/4\pi\sigma \quad (2.28)$$

is the efficiency of the contact recombination.[13,8,15]

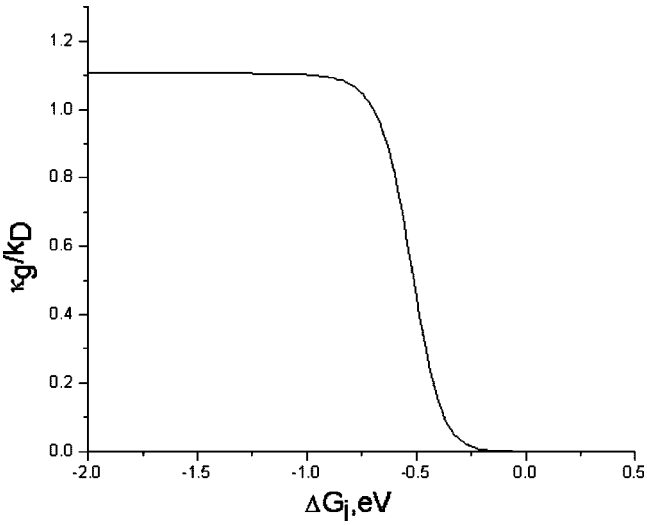

Figure 2. FEG law for the geminate Stern−Volmer constant for the three different situations: (1) no recombination and exciplex formation ($k_c = k_t = k_a = 0$), (2) no triplet and exciplex formation ($k_t = k_a = 0$, $k_c^0 = 10^6$ Å^3/ns), (3) no exciplex formation ($k_a = 0$, $k_c^0 = k_t^0 = 10^6$ Å^3/ns). All of the curves are not distinguishable.

E. FEG for the Forward Electron Transfer. The free-energy dependence of the fluorescence quantum yield η and the charge separation yield φ are the most popular subjects of the numerous experimental investigations.[8,15] The former is used for calculation of the Stern−Volmer constant from eq 2.3 and its comparison with the theoretical predictions.

If we neglect recombination to the exciplex and the ground state, setting $k_a = k_c = 0$, the Stern−Volmer constant (eq 2.17) has to increase so that

$$\frac{\kappa_i}{\kappa_g} \le 1 + \frac{\kappa_i}{K_{eq}k_{esc}}$$

As seen from eq 2.20,

$$k_{esc} \ge k_D \quad \text{while} \quad k_i \le k_D(1 + \sqrt{\tau_d/\tau_A})$$

Hence

$$\frac{\kappa_i}{\kappa_g} \le 1 + e^{\Delta G_i/T}(1 + \sqrt{\tau_d/\tau_A})$$

and everywhere in the exergonic region ($\Delta G_i < 0$)

$$\kappa_g = \kappa_i = \frac{k_F k_D(1 + \sqrt{\tau_d/\tau_A})}{k_F + k_D(1 + \sqrt{\tau_d/\tau_A})} = \begin{cases} k_D(1 + \sqrt{\tau_d/\tau_A}) & \text{diffusional plateau} \\ k_F = k_F^0 e^{-[(\Delta G_i + \lambda)^2]/4\lambda T} & \text{kinetic control} \end{cases} \quad (2.29)$$

The free-energy dependence of κ_g calculated from general formula (eq 2.17) and shown in Figure 2 actually consists of the diffusional plateau and descending branch that belongs to $k_F(\Delta G_i)$. The former is really flat in the contact approximation, though shifted up from the line $\kappa_g = k_D = 4\pi\sigma D$, due to the transient term $\sqrt{(\tau_d/\tau_A)} = \sqrt{(\sigma^2/D\tau_A)}$. In the log plot, the descending branch of κ_g looks like a downhill line, which is indifferent to either recombination or exciplex formation. When $K_{eq}k_{esc} \gg \kappa_i$, the RIP separation alone is so fast that it makes ionization irreversible (with or without help of other RIP reactions).

Because this is usually the case, the forward electron transfer was considered irreversible in the vast majority of works devoted to the so-called Rehm−Weller paradox.[13,15,16] On the contrary, the backward transfer to the ground-state, which is not limited by diffusion (no plateau in principle), always confirmed the bell-shaped FEG law (eq 2.14) for recombination efficiency Z originated mainly from k_c. The deviation from this law will be discussed below.

F. FEG Law for the Backward Electron Transfer. The quantum yield of charge separation from contact distance is usually presented by the relationship,

$$\varphi = \frac{1}{1 + Z/D} \quad (2.30)$$

where the recombination efficiency Z can be specified using the general expression for φ given in eq 2.25:

$$\frac{Z}{D} = \frac{z}{D} + \frac{k_{exc}}{k_D} + \frac{3}{4}\sqrt{4k_s\tau_d}\frac{[(k_D k_t)/(k_D + k_{-t})] - k_c}{[(k_D k_t)/(k_D + k_{-t})] + k_D[1 + \sqrt{4k_s\tau_d}]} \quad (2.31)$$

where z was defined in (2.28). This formula is equivalent to eq (3.19) obtained in ref.[17] for the irreversible triplet formation:

$$\frac{Z}{D} = \frac{z}{D} + \frac{3}{4}\frac{(k_t - k_c)\sqrt{4k_s\tau_d}}{k_t + k_D[1 + \sqrt{4k_s\tau_d}]} \quad \text{at} \quad k_{-t} = k_{exc} = 0 \quad (2.32)$$

This expression accounts for the interference of two recombination channels: via singlet and triplet RIP. If the latter is the only one acting, then

$$Z = \frac{3k_t}{16\pi\sigma}\frac{\sqrt{4k_s\tau_d}}{1 + \sqrt{4k_s\tau_d} + k_t/k_D}$$

is exactly the same as in eq 3.22 of ref 17.

As a matter of fact, the spin-conversion during the encounter is often negligible. When it is induced by HFI in radicals, the best fit with real data appears at $k_s = A/32$ where A is the effective HFI constant.[13,18] At $A = 10^8$ s^{-1} and $\tau_d = 2$ ns, we have $\sqrt{(4k_s\tau_d)} = 3 \times 10^{-2} \ll 1$. Setting it to zero, we get from eq 2.25:

$$\varphi = \frac{k_D}{k_c + k_{exc} + k_D} \quad \text{or} \quad \frac{Z}{D} = \frac{k_c + k_{exc}}{k_D} \quad (2.33)$$

According to eq 2.18 after exergonic ionization

$$\frac{Z}{D} = \frac{z}{D} + \frac{v\exp(-\Delta G_{RIP}/T)}{4\pi\sigma D\tau_e} \quad (2.34)$$

where $\Delta G_{RIP} = \Delta G_{exc} - \Delta G_i$.

In the simplest model of a single channel phononless electron transfer, the recombination efficiency,

$$z = \frac{k_c}{4\pi\sigma} = z_0 \exp\left(-\frac{(\Delta G_r + \lambda)^2}{4\lambda T}\right) \quad (2.35)$$

This Gaussian, $z(\Delta G_r)$, has the maximum at $\Delta G_r = -(\Delta G_I + E_S) = -\lambda$ and dominates nearby (Figure 3). The second term in the rhs of eq 2.34 represents the exciplex contribution in the total efficiency Z within the endergonic region. It results in the small deviation of this quantity from z in the vicinity of the resonance ($\Delta G_I \lesssim 0$). There and only there this contribution is dominant (insert), thus manifesting about the formation of the

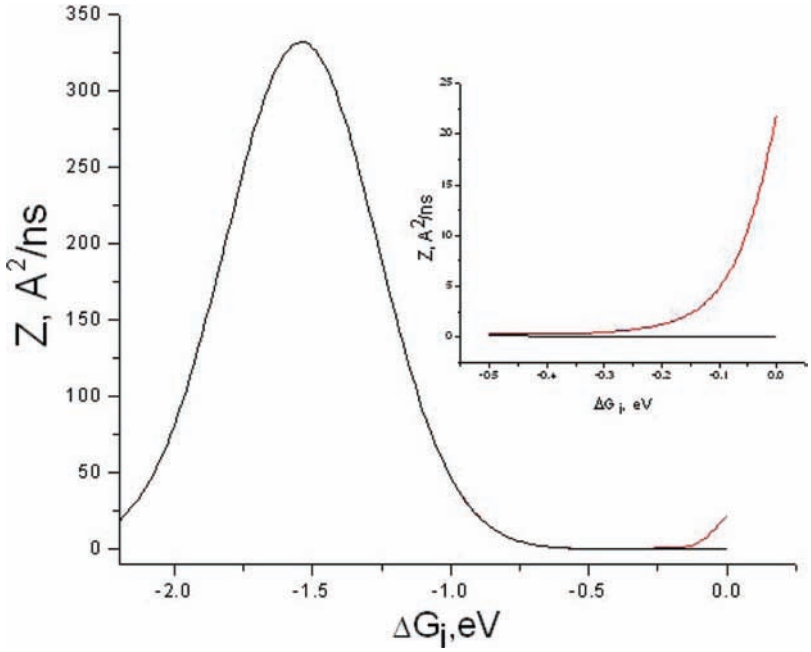

Figure 3. FEG law for the recombination efficiency with (red line) and without exciplex formation (black line). The exergonic branch of exciplex recombination peak near $\Delta G_i \approx 0$ is shown in the insert.

exciplex by exciton quenching. Unfortunately, the experimental study of the FEG law in recombination is never extended so far from maximum.

If we turn to the charge separation quantum yield (eq 2.30) from where Z was extracted (part a of Figure 4), the exciplex formation manifests itself more clearly: by the sharp descending branch near $\Delta G_i = 0$. However, φ is a quantity that is not measured but calculated. The initial information comes from the free ions quantum yield ϕ, which is the straightforward measured quantity. It also has even a sharper descending (right) branch in part c of Figure 4 but of a different origin. This downhill branch is indifferent to whether the exciplex is formed or not. It reproduces the similar branch of $\psi = 1 - \eta$ (part b of Figure 4). The free ions do not disappear because of additional recombination; they just do not appear at all because $\psi \rightarrow 0$ ($\eta \rightarrow 1$) in the region of kinetic control ionization (part b of Figure 4). This effect eliminated in $\varphi = \phi/\psi$ is clearly seen in ϕ (part c of Figure 4). A similar effect is also seen at the opposite exergonic side of the same figure. It can hardly appear in the real experiment because of the Rehm−Weller paradox: the diffusional plateau $\kappa_g \approx k_D$ is usually too long (due to vibronic and electronic excitations of products). This makes $\psi \approx c\kappa_g\tau_A = \text{const}$, preventing the actual reduction of ϕ, with increasing exergonicity of forward electron transfer.

Even the right descending branch of φ "has probably been found for the first time" by using anthracenecarbonitriles as the electron-accepting fluorescer and 1,4-diphenyl-1,3-butadienes as the electron donating quencher (Figure 2 in ref 19). In other works of the same group,[20−22] only the opposite effect was indicated: the minimum in $k_c \equiv k_b$ near almost resonant recombination, $-\Delta G_r = \Delta G_i + E_S \approx 0$, not at resonant ionization, $-\Delta G_i \approx 0$. In all of these works, the authors stressed that "the yield of the ground-state RIP is unity",[20] that is $\psi = 1$ because "the fluorescence quenching is induced by long-distance (outer-sphere) electron transfer for producing" the RIP.[20] For this reason, they identify ϕ and φ, setting

$$\phi \equiv \varphi = \frac{k_{esc}}{k_{esc} + k_b} \tag{2.36}$$

where

$$k_{esc} = \frac{3Dr_c}{r_q^3[\exp(r_c/r_q) - 1]} \rightarrow 3D/r_q^2 \quad \text{at} \quad r_c = 0 \tag{2.37}$$

This is definitely not true because the concentration dependent,

$$\psi = 1 - \eta = \frac{c\kappa_g\tau_A}{1 + c\kappa_g\tau_A} \tag{2.38}$$

is less than 1 at any concentration used in these experiments, and κ_g is not a constant even at long distance transfer. Therefore, k_b tabulated there and shown in Figure 5 can only be used for the restoration of $\phi(\Delta G_r)$ from eqs 2.36 and 2.37.

Using the data represented in part A of Figure 5, we obtained $\phi(\Delta G_r)$ shown by black squares in part a of Figure 6. The corresponding values of ψ shown in the same figure by red squares were calculated using κ_g measured in the same work,[20] though in a much narrower interval. Only within this interval we could restore

$$\varphi = \frac{\phi}{\psi} = \frac{1}{1 + Z/D} \tag{2.39}$$

The results shown in part b of Figure 6 as well as $Z/D \equiv k_c/k_D$ found from it (part c of Figure 6) are fitted by the ideal FEG law for k_c given by eq 2.14 with 2 varying parameters shown to be $k_c^0/k_D = 64.8$ and $\lambda = 1.87$ eV.

Unfortunately, we can not judge whether the extremum near zero ΔG_r seen in part A of Figure 5 and in part a of Figure 6 for k_b and ϕ is or is not present in Z because of the lack of ψ points in this region. The situation is even worse with the similar peculiarity at the opposite side in part B of Figure 5. The authors of this work did not present any data about $\kappa_g \equiv k_q$, although the latter was announced to be present in Table 1 of ref 19. Therefore, the question whether this is the manifestation of exciplex formation (as they stated) or just the trivial cutoff by $\psi(\Delta G_i)$ like in part c of Figure 4 remains open.

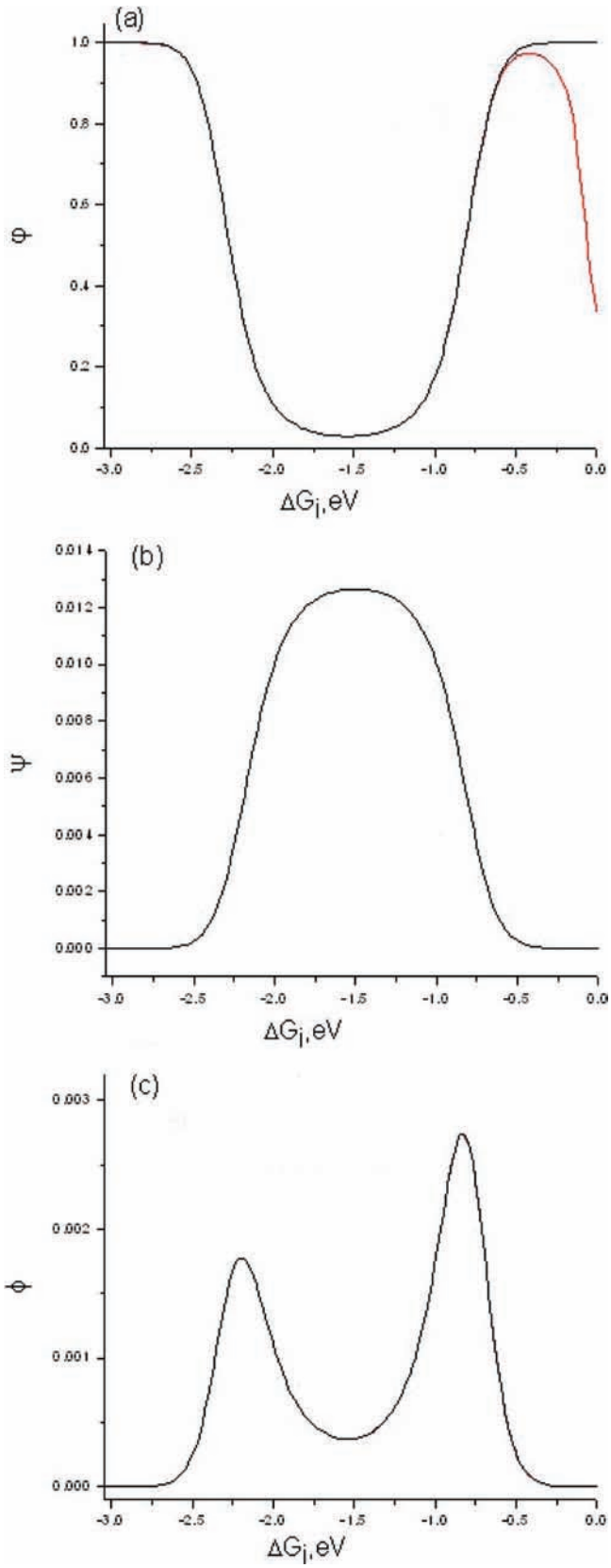

Figure 4. Free-energy dependence of (a) the charge separation yield φ, (b) ion formation yield ψ, and (c) free ion yield ϕ with (red lines) and without (black lines) exciplex formation.

III. Stationary Excitation

A. IET Accounting for the Bulk Reactions. The general kinetic equations for the reaction Scheme 2 (Figure 1) includes both the geminate and the bulk reactions:

$$\frac{\mathrm{d}}{\mathrm{d}t}N^* = -c\int_0^t R_{11}(t-\tau)N^*(\tau)\,\mathrm{d}\tau + \int_0^t R_{12}(t-\tau)N^e(\tau)\,\mathrm{d}\tau + \int_0^t R_{13}(t-\tau)P^2(\tau)\,\mathrm{d}\tau + c\int_0^t R_{14}(t-\tau)N_T(\tau)\,\mathrm{d}\tau - \frac{N^*}{\tau_A} + IN$$

$$\frac{\mathrm{d}}{\mathrm{d}t}N^e = c\int_0^t R_{21}(t-\tau)N^*(\tau)\,\mathrm{d}\tau - \int_0^t R_{22}(t-\tau)N^e(\tau)\,\mathrm{d}\tau + \int_0^t R_{23}(t-\tau)P^2(\tau)\,\mathrm{d}\tau + c\int_0^t R_{24}(t-\tau)N^T(\tau)\,\mathrm{d}\tau - \frac{N^e}{\tau_e}$$

$$\frac{\mathrm{d}}{\mathrm{d}t}P = c\int_0^t R_{31}(t-\tau)N^*(\tau)\,\mathrm{d}\tau + \int_0^t R_{32}(t-\tau)N^e(\tau)\,\mathrm{d}\tau - \int_0^t R_{33}(t-\tau)P^2(\tau)\,\mathrm{d}\tau + c\int_0^t R_{34}(t-\tau)N^T(\tau)\,\mathrm{d}\tau$$

$$\frac{\mathrm{d}}{\mathrm{d}t}N^T = c\int_0^t R_{41}(t-\tau)N^*(\tau)\,\mathrm{d}\tau + \int_0^t R_{42}(t-\tau)N^e(\tau)\,\mathrm{d}\tau + \int_0^t R_{43}(t-\tau)P^2(\tau)\,\mathrm{d}\tau - \int_0^t R_{44}(t-\tau)N^T(\tau)\,\mathrm{d}\tau$$

At stationary illumination $I = I_0 = \mathrm{const}$, all of the quantities have their stationary values reached at $t \to \infty$ that obey the following set of algebraic equations:

$$0 = -c\tilde{R}_{11}(0)N^*_{st} + \tilde{R}_{12}(0)N^e_{st} + \tilde{R}_{13}(0)P^2_{st} + c\tilde{R}_{14}(0)N^T_{st} - \frac{N^*_{st}}{\tau_A} + I_0N \quad (3.1a)$$

$$0 = c\tilde{R}_{11}(0)N^*_{st} - \tilde{R}_{22}(0)N^e_{st} + \tilde{R}_{23}(0)P^2_{st} + c\tilde{R}_{24}(0)N^T_{st} - \frac{N^e_{st}}{\tau_e} \quad (3.1b)$$

$$0 = c\tilde{R}_{31}(0)N^*_{st} + \tilde{R}_{32}(0)N^e_{st} - \tilde{R}_{33}(0)P^2_{st} + c\tilde{R}_{34}(0)N^T_{st} \quad (3.1c)$$

$$0 = c\tilde{R}_{41}(0)N^*_{st} + \tilde{R}_{42}(0)N^e_{st} + \tilde{R}_{43}(0)P^2_{st} - \tilde{R}_{44}(0)N^T_{st} \quad (3.1d)$$

They can be easily solved providing all of the necessary information for the different measurable quantities.

They are the yields of the stationary luminescence of the excitation and exciplex:

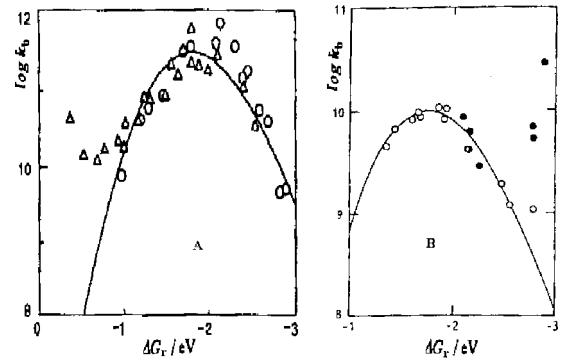

Figure 5. k_b dependence on the recombination free energy for the systems studied in ref 20 (A) and ref 19 (B). The deviations from the FEG law parabolas (solid lines) are at the opposite sides: (A) at $\Delta G_r \approx 0$ ($-\Delta G_i \sim E_S$) and (B) at $\Delta G_r \approx -E_S$ ($\Delta G_i \approx 0$). Only the last could be related to exciplex formation.

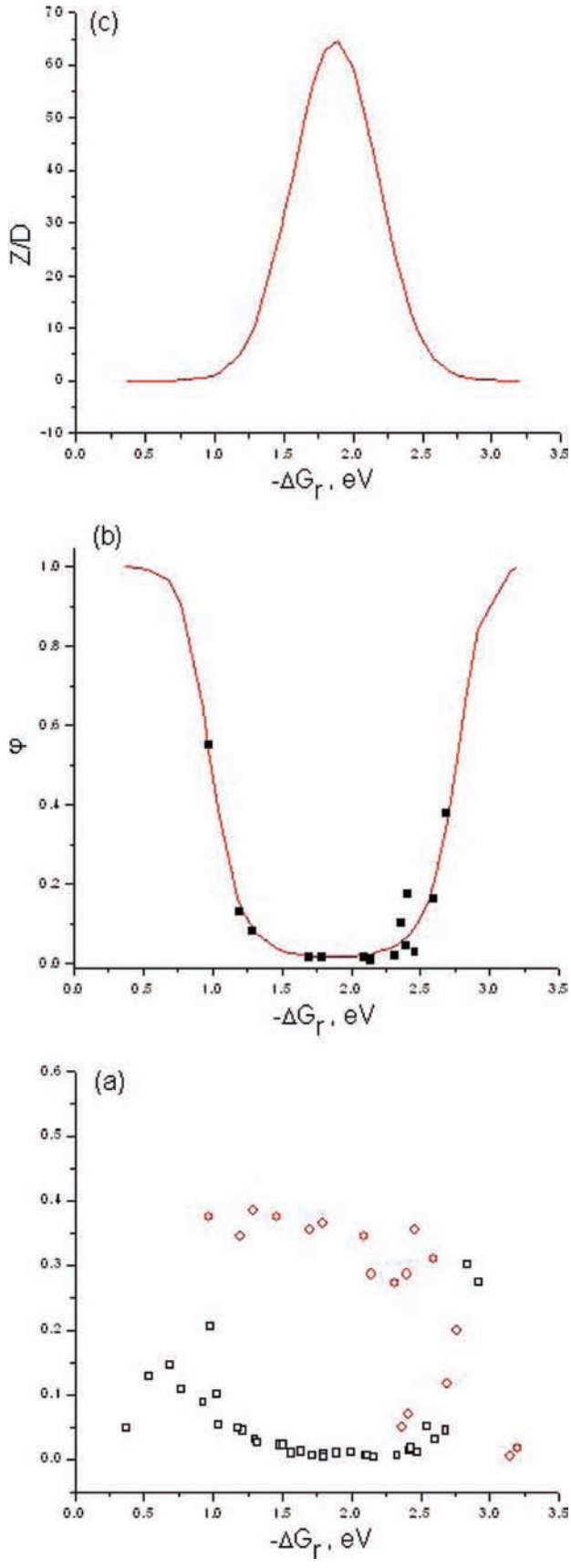

Figure 6. Analysis of the FEG law in systems A studied in ref 20. (a) The free-energy dependence of the free ion yield ϕ calculated with k_b from part A of Figure 5 (black squares) and initial yield of ions ψ (red squares), calculated with the available κ_g from the same work. (b) The charge separation yield $\varphi = \phi/\psi = 1/(1 + Z/D)$ and (c) the ratio $Z/D \equiv k_c/k_D$ obtained by fitting to them the simplest Marcus FEG law (eq 2.14) (red lines).

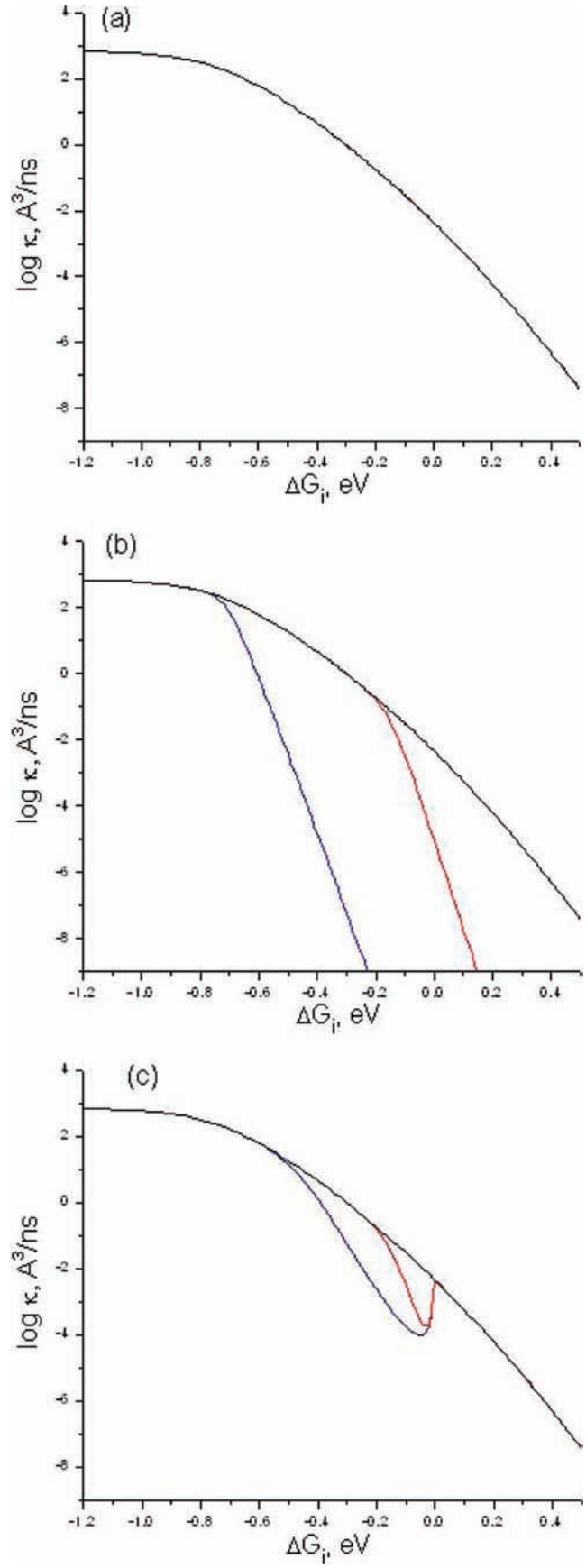

Figure 7. FEG law for the stationary Rehm−Weller constant κ (Å^3/ns) at $k_c^0/k_D = 10^{-8}$ (blue), 10^{-1} (red), and ∞ (black) when the exciplex is (a) strongly bounded ($V = 10^{-2}$ eV); (c) weakly bounded ($V = 10^{-4}$ eV); or (b) does not exist at all ($k_a = 0$). The rest of the parameters are: $k_F^0 = 1.4 \times 10^5$ Å^3/ns; $\sigma = 5$ Å, $D = 10$ Å^2 /ns, $r_c = 12$ Å, $\tau_A = 1$ ns, $k_s = k_t = 0$.

$$\eta_{st} = \frac{N^*_{st}}{I_0 N \tau_A} = \frac{1}{1 + c\tau_A \kappa} \tag{3.2a}$$

$$\eta^e_{st} = \frac{N^e_{st}}{I_0 N \tau_e} \tag{3.2b}$$

where

$$\begin{aligned}\kappa = \tilde{R}_{11} - [\{&\tilde{R}_{12}\tilde{R}_{21}(\tilde{R}_{33}\tilde{R}_{44} - \tilde{R}_{34}\tilde{R}_{43}) + \\ &\tilde{R}_{13}\tilde{R}_{31}(\tilde{R}_{22}\tilde{R}_{44} - \tilde{R}_{24}\tilde{R}_{42}) + \\ &\tilde{R}_{14}\tilde{R}_{41}(\tilde{R}_{22}\tilde{R}_{33} - \tilde{R}_{23}\tilde{R}_{32}) + \\ &\tilde{R}_{22}(\tilde{R}_{14}\tilde{R}_{31}\tilde{R}_{43} + \tilde{R}_{13}\tilde{R}_{34}\tilde{R}_{41}) + \\ &\tilde{R}_{33}(\tilde{R}_{12}\tilde{R}_{24}\tilde{R}_{41} + \tilde{R}_{14}\tilde{R}_{21}\tilde{R}_{42}) + \\ &\tilde{R}_{44}(\tilde{R}_{13}\tilde{R}_{21}\tilde{R}_{32} + \tilde{R}_{12}\tilde{R}_{23}\tilde{R}_{31}) + \\ &\tilde{R}_{12}\tilde{R}_{23}\tilde{R}_{34}\tilde{R}_{41} + \tilde{R}_{12}\tilde{R}_{24}\tilde{R}_{31}\tilde{R}_{43} + \\ &\tilde{R}_{13}\tilde{R}_{24}\tilde{R}_{32}\tilde{R}_{41} + \tilde{R}_{13}\tilde{R}_{21}\tilde{R}_{34}\tilde{R}_{42} + \\ &\tilde{R}_{14}\tilde{R}_{23}\tilde{R}_{31}\tilde{R}_{42} + \tilde{R}_{14}\tilde{R}_{21}\tilde{R}_{32}\tilde{R}_{43}\}\tau_e + \\ &(\tilde{R}_{14}\tilde{R}_{33}\tilde{R}_{41} + \tilde{R}_{13}\tilde{R}_{34}\tilde{R}_{41} + \tilde{R}_{14}R_{31}R_{43} + \\ &\tilde{R}_{13}R_{31}R_{44})]/[\tilde{R}_{33}\tilde{R}_{44} - \tilde{R}_{34}\tilde{R}_{43} + \\ &\{\tilde{R}_{22}\tilde{R}_{33}\tilde{R}_{44} - \tilde{R}_{24}\tilde{R}_{33}\tilde{R}_{42} - \tilde{R}_{23}\tilde{R}_{34}\tilde{R}_{42} - \\ &\tilde{R}_{24}\tilde{R}_{32}\tilde{R}_{43} - \tilde{R}_{22}\tilde{R}_{34}\tilde{R}_{43} - \tilde{R}_{23}\tilde{R}_{32}\tilde{R}_{44}\}\tau_e] \end{aligned} \tag{3.3}$$

The exciplex quantum yield is related to the fluorescence one as follows:

$$\begin{aligned}\frac{\eta^e_{st}}{c\eta_{st}} = \tau_A[&\tilde{R}_{21}(\tilde{R}_{33}\tilde{R}_{44} - \tilde{R}_{34}\tilde{R}_{43}) + \tilde{R}_{23}(\tilde{R}_{31}\tilde{R}_{44} + \tilde{R}_{34}\tilde{R}_{41}) + \\ &\tilde{R}_{24}(\tilde{R}_{31}\tilde{R}_{43} + \tilde{R}_{33}\tilde{R}_{41})]/[\tilde{R}_{33}\tilde{R}_{44} - \tilde{R}_{34}\tilde{R}_{43} + \\ &\{\tilde{R}_{33}(\tilde{R}_{22}\tilde{R}_{44} - \tilde{R}_{24}\tilde{R}_{42}) - \tilde{R}_{32}(\tilde{R}_{23}\tilde{R}_{44} + \tilde{R}_{24}\tilde{R}_{43})) - \\ &\tilde{R}_{34}(\tilde{R}_{23}\tilde{R}_{42} + \tilde{R}_{22}\tilde{R}_{43})\}\tau_e] \end{aligned} \tag{3.4}$$

The measurements of the electro-conductivity can provide us with a stationary carrier density P_{st}, whereas the fluorescence or light absorption of the triplets is proportional to their density N^T_{st}. Both of these densities are also expressed via integral kernels at $s = 0$:

$$\begin{aligned}\frac{P^2_{st}}{cN^*_{st}} = [&\tilde{R}_{31}\tilde{R}_{44} + \tilde{R}_{34}\tilde{R}_{41} + \{\tilde{R}_{31}(\tilde{R}_{22}\tilde{R}_{44} - \tilde{R}_{24}\tilde{R}_{42}) + \\ &\tilde{R}_{32}(\tilde{R}_{21}\tilde{R}_{44} + \tilde{R}_{24}\tilde{R}_{41}) + \\ &\tilde{R}_{34}(\tilde{R}_{22}\tilde{R}_{41} + \tilde{R}_{21}\tilde{R}_{42})\}\tau_e]/[\tilde{R}_{33}\tilde{R}_{44} - \tilde{R}_{34}\tilde{R}_{43} + \\ &\{\tilde{R}_{33}(\tilde{R}_{22}\tilde{R}_{44} - \tilde{R}_{24}\tilde{R}_{42}) - \tilde{R}_{32}(\tilde{R}_{23}\tilde{R}_{44} + \tilde{R}_{24}\tilde{R}_{43})) - \\ &\tilde{R}_{34}(\tilde{R}_{23}\tilde{R}_{42} + \tilde{R}_{22}\tilde{R}_{43})\}\tau_e] \end{aligned} \tag{3.5}$$

$$\begin{aligned}\frac{N^T_{st}}{N^*_{st}} = [&\tilde{R}_{31}\tilde{R}_{43} + \tilde{R}_{33}\tilde{R}_{41} + \{\tilde{R}_{41}(\tilde{R}_{22}\tilde{R}_{33} + \\ &\tilde{R}_{23}\tilde{R}_{32}) + \tilde{R}_{42}(\tilde{R}_{21}\tilde{R}_{33} + \tilde{R}_{23}\tilde{R}_{31}) + \\ &\tilde{R}_{43}(\tilde{R}_{21}\tilde{R}_{32} + \tilde{R}_{22}\tilde{R}_{31})\}\tau_e]/[\tilde{R}_{33}\tilde{R}_{44} - \tilde{R}_{34}\tilde{R}_{43} + \\ &\{\tilde{R}_{33}(\tilde{R}_{22}\tilde{R}_{44} - \tilde{R}_{24}\tilde{R}_{42}) - \tilde{R}_{32}(\tilde{R}_{23}\tilde{R}_{44} + \tilde{R}_{24}\tilde{R}_{43})) - \\ &\tilde{R}_{34}(\tilde{R}_{23}\tilde{R}_{42} + \tilde{R}_{22}\tilde{R}_{43})\}\tau_e] \end{aligned} \tag{3.6}$$

B. Contact Approximation. In the contact approximation, all additional kernels are specified as those defined in eqs 2.12a:

$$R_{14} = \frac{k_B k_{-t}}{3k_F k_t} R_{41} \qquad R_{13} = \frac{k_B}{4k_F} R_{31} \tag{3.7a}$$

$$R_{23} = \frac{k_a}{4k_d} R_{32} \qquad R_{24} = \frac{k_a k_{-t}}{3k_d k_t} R_{42} \tag{3.7b}$$

$$\tilde{R}_{34} = \frac{4k_{-t}}{Y}\{[1 + g_3(k_a + k_c)](1 + k_F g_1) + k_B g_3\} = \frac{4k_{-t}}{3k_t}\tilde{R}_{43} \tag{3.7c}$$

$$\begin{aligned}\tilde{R}_{33} = \frac{1}{Y}[&k_t((1 + k_f g_1)(3 + 4g_3(k_a + k_c)) + 4k_b g_3) + \\ &((k_a + k_c)(1 + k_f g_1) + k_b)(1 + g_5 k_{-t})] \end{aligned} \tag{3.7d}$$

$$\tilde{R}_{44} = \frac{k_{-t}}{Y}[(4 + (3g_3 + g_4)(k_a + k_c))(1 + k_f g_1) + (3g_3 + g_4)k_b] \tag{3.7e}$$

where g_i is defined in eqs 2.15 and 2.16, whereas Y is given by eq 2.12h.

In this approximation, the yields are given by the following formulas:

$$\frac{1}{\kappa} = \frac{1}{\kappa_i} + \frac{1}{K_{eq}(k_c + k_{exc})} \tag{3.8}$$

$$\eta^e_{st} = (1 - \eta_{st})\frac{k_{exc}}{k_c + k_{exc}} \tag{3.9}$$

whereas the charge and triplet densities are

$$P^2_{st} = \frac{4c\kappa_i N^*_{st}}{k_c + k_{exc} + \kappa_i / K_{eq}} \tag{3.10}$$

$$cN^T_{st} = \frac{3k_t}{4k_{-t}} P^2_{st} \tag{3.11}$$

where

$$N^*_{st} = \frac{I_0 N \tau_A}{1 + c\kappa\tau_A}$$

We shall restrict further discussion to only the fluorescence quantum yield, which is determined by the Stern−Volmer constant $\kappa \neq \kappa_g$. The main difference between these quantities is seen from the comparison of eqs 3.8 and 2.17. The stationary constant κ does not contain k_{esc}, which dominates in κ_g. Under stationary conditions, all of the separated RIPs recombine later on in the bulk to the precursors. Because of this, the stationary constant is much more sensitive to the alternative mechanisms of RIP dissipation: irreversible recombination to the ground state (k_c) and reversible exciplex formation (k_{exc}). Only they determine the FEG law peculiar to the stationary obtained Stern−Volmer constant (eq 3.8) that can be represented in the following form:

$$\frac{1}{\kappa} = \frac{1}{k_F} + \frac{1}{k_D(1 + \sqrt{\tau_d/\tau_A})} + \frac{k_B}{k_F(k_c + k_{exc})} \tag{3.12}$$

Here, the first term represents the kinetic ionization, which obeys the original (parabolic) Marcus FEG law.[23] The second one gives the diffusional plateau corrected for the transient effect. The latter obtained experimentally by Rehm and Weller[16] cuts the top of Marcus parabola. The theoretical description of this phenomenon first given in ref 24 was many times reconsidered in attempts to solve the Rehm−Weller paradox: why the plateau extends too far into the exergonic region. The final resolution of this paradox was given in our recent work.[25]

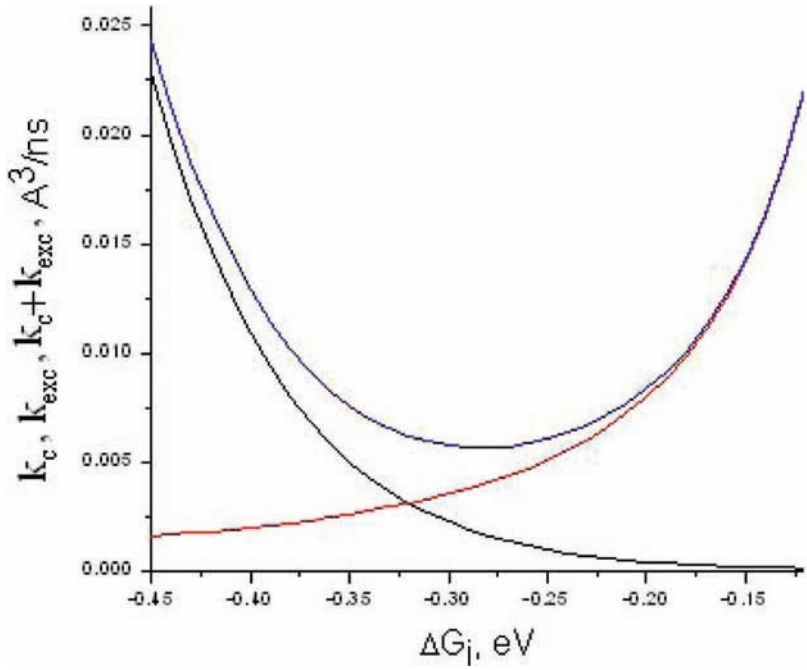

Figure 8. RIP recombination to the ground state, $k_c(\Delta G_i)$ (black line), and to the exciplex, $k_{exc}(\Delta G_i)$ (red line), and their sum (blue line) at ($V = 10^{-2}$ eV). The rest of the parameters are the same as in Figure 7.

At the same time, the descending endergonic branch is always ascribed to the irreversible kinetic reaction of the forward electron transfer belonging to $k_F(\Delta G_i)$. Only the recent experiments of Jacques and Allonas[6] demonstrated what they called a "multiple Rehm−Weller effect": the descending branch of the FEG curve is not a unique (kinetic) stage of the reaction. There are a number of them belonging to the different families of the reactants. The effect was recently ascribed to the last term in eq 3.12. When it is dominant, the reversible reaction is limited neither by ionization nor by diffusion: it is controlled by recombination of the charged products to either the ground or exciplex state. In the absence of the latter ($k_{exc} = 0$), this phenomenon was discussed a few times,[17,23] assuming that recombination is different in different reactant families and the rate of it, k_c, determines the slope of the descending branch in each of them (part b of Figure 7).

Here, we only have to extend this analysis taking into account the exciplex formation as a parallel recombination channel. The rate of recombination to exciplex monotonously increases with ΔG_i, whereas the competing recombination to the ground-state decreases with $\Delta G_I > -\lambda$ (Figure 8). The sum of them passes through the minimum, which is lower the smaller V becomes. In the vicinity of this extremum, the double-channel recombination controls the quenching if its minimal rate is low enough. Otherwise it does not play any role. In Figure 7, we compare the FEG law for energy quenching in the absence of exciplex formation, $k_a = 0$ (part b of Figure 7), and in the presence of it ($k_a \gg k_D$): at large V (part a of Figure 7) and at small V (part c of Figure 7). At large V, even the minimal recombination is so fast that it completely exhausts the RIP state, making its formation irreversible, that is controlled by either diffusional or kinetic ionization (part a of Figure 7). At small V, the minimum of the RIP recombination is too low and controls the reaction in its vicinity, but to the left of it dominates the recombination to the ground state, whereas the exciplex formation dominates to the right of it. Generally speaking, the exciplex peculiarity in the stationary obtained κ can be hardly seen but in κ_g obtained in pulse experiments it is almost not seen at all (Figure 2).

IV. Conclusions

Using the Weller Scheme II for the reversible exciplex formation from the RIP, we found that there is no deviation from the canonical Rehm−Weller picture in the case of δ-pulse excitation (Figure 2) but it could be obtained as the local peculiarity in the free-energy dependence of stationary Stern−Volmer constant (part c of Figure 7). This feature can be used for the identification of Scheme II because in Scheme I studied earlier[9,18] the FEG law is qualitatively different. Instead of the abrupt cut of the diffusional plateau by the kinetic branch of κ_i, there is the smooth (quasi-exponential) decrease of κ with ΔG_i, representing the straightforward exciplex formation from the excited reactants passing the RIP.

We also analyzed some anomalies in the FEG law for the "backward rate constant" found from the free ion yield ϕ in both the exergonic and endergonic descending branches.[19−21] This was shown to be an artifact resulting from the superposition of the ionization and charge separation yields ($\phi = \psi\varphi$). Only the latter (φ) has a single objective deviation from FEG in the endergonic side caused by the exciplex formation. Unfortunately, the charge separation yield can not be extracted from the reported experimental data due to the lack of the Stern−Volmer constants determining the ionization yield $\psi = 1 - \eta$.

In line with κ and φ, the exciplex formation yield η^e was also studied at any light excitation as well as the yield of the triplet products resulting from the RIP recombination assisted by spin conversion or bulk encounters of free ions. The stationary concentrations of the triplet and ions were also specified in the contact approximation.

In the present theory, the exciplex formation occurs at each contact between the reactants. In such a case, the reaction sphere of contact radius σ can be considered as a black one and the reaction controlled by diffusion proceeds with the rate constant $k_D = 4\pi\sigma D$. However, the reactants that are not spherically isotropic should be considered as the white spheres with the reactive spots on them, which occupy just the f part of the total spherical surface. In the case of the fast radical reactions, the spots are black but the reaction rates being proportional to

diffusion are smaller than k_D. These reactions are known as the "pseudo-diffusional" ones.[29] The numerous recontacts and spherical rotation of the partners during encounter expend the effective reaction area making the rate constant equal to $f_{eff}k_D$. The calculation of $f_{eff}(D) < 1$ is a special problem that has been successfully solved in a number of earlier works[27,28,30] and reviewed in ref 29. In a few recent works[9,18] including the present one, we ignored this problem for the sake of simplicity setting $f = 1$ but the sperical anisotropy of exciplex formation can be included into IET consideration as well as in the theory of the free radical reactions.

As a matter of fact, the electron transfer is a distant reaction proceeding with the rate $W_F(r)$ at any reactant separation. Under diffusion control, the stationary ionization occurs mainly at the effective (diffusion-dependent) radius $R_Q(D)$. It is larger than the contact one (σ), where the exciplexes are born according to the Weller Scheme I.[9] At relatively slow diffusion and large enough W_F, the reactants are ionized before reaching the contact distance so that Scheme II dominates in Scheme I. However, the situation changes to opposite with fastening diffusion. To study the simultaneous action of both competing schemes, one has to use distant instead of contact theory of ionization. This is what has to be done next, at least numerically.

Acknowledgment. The authors are grateful to the Karyn Kupcinet International Science School for Overseas Students and the head of the Chem. Phys. Dept. of WIS, Prof. S. Vega, for the opportunity of providing this collaboration together in Israel.

References and Notes

(1) Weller, A. *Zeitschrift für Physikalische Chemie Neue Folge* **1982**, *130*, 129.
(2) Weller, A.; Staerk, H.; Treichel, R. *Faraday Discuss. Chem.* **1984**, *78*, 271.
(3) Schulten, K.; Staerk, H.; Weller, A.; Werner, H.-J.; Nickel, B. *Zeitschrift für Physikalische Chemie Neue Folge* **1976**, *101*, 371.
(4) Foll, R. E.; Kramer, H. E. A.; Steiner, U. E. *J. Phys. Chem.* **1990**, *94*, 2476.
(5) Gould, I. R.; Young, R. H.; Mueller, L. J.; Albrecht, A. C.; Farid, S. *J. Am. Chem. Soc.* **1994**, *116*, 8188.
(6) Dossot, M.; Allonas, H. *Chem.—Eur. J.* **2005**, *11*, 1763.
(7) Kuzmin, M. *J. Photochem. Photobiol., A* **1996**, *102*, 51.
(8) Burshtein, A. I. *Adv. Chem. Phys.* **2000**, *114*, 419.
(9) Petrova, M. Burshtein A. I. J. Phys. Chem. A **2008**, *112*, 13343.
(10) Burshtein, A. I.; Yakobson, B. I. *Int. J. Chem. Kinet.* **1980**, *XII*, p. 261.
(11) Burshtein, A. I.; Doktorov, A. B.; Morozov, A. V. *Chem. Phys.* **1986**, *104*, 1.
(12) Lukzen, N. N.; Pedersen, J. B.; Burshtein, A. I. *J. Phys. Chem. A* **2005**, *109*, 11926.
(13) Burshtein A. I. Adv. Phys. Chem. **2009**, DOI: 10.1155/2009/214219.
(14) Ivanov, K. L.; Lukzen, N. N.; Doktorov, A. B.; Burshtein, A. I. *J. Chem. Phys.* **2001**, *114*, 1754.
(15) Burshtein, A. I. *Adv. Chem. Phys.* **2004**, *129*, 105.
(16) Rehm, D.; Weller, A. *Israel J. Chem.* **1970**, *8*, 259.
(17) Burshtein, A. I.; Ivanov, K. L. *Phys. Chem. Chem. Phys.* **2002**, *4*, 4115. Appendix available online: http://www.rsc.org/suppdata/cp/b2/b201784a/.
(18) Ivanov, A. I. Burshtein A. I. J. Phys. Chem. A. **2008**, *112*, 6392.
(19) Kikuchi, K.; Takahashi, Y.; Hoshi, M.; Niva, T.; Katagiri, T.; Miyashi, T. *J. Phys. Chem.* **1991**, *95*, 2378.
(20) Niwa Inada, T.; Kikuchi, K.; Takahashi, Y.; Ikeda, H.; Miyashi, T. *J. Photochem. Photobiol., A* **2000**, *137*, 93.
(21) Kikuchi, K.; Katagiri, T.; Niwa, T.; Takahashi, Y.; Suzuki, T.; Ikeda, H.; Miyashi, T. *Chem. Phys. Lett.* **1992**, *193*, 155.
(22) Niwa, T.; Kikuchi, K.; Matsusita, N.; Hayashi, M.; Katagiri, T.; Takahashi, Y.; Miyashi, T. *J. Phys. Chem.* **1993**, *97*, 11960.
(23) Marcus, R. A. *J. Chem. Phys.* **1956**, *24*, 966. *ibid* **43**, 679 (1965).
(24) Marcus, R. A.; Siders, P. *J. Phys. Chem.* **1982)** , *86*, 622(.
(25) Burshtein, A. I.; Ivanov, A. I. *PCCP* **2007**, *9*, 396.
(26) Burshtein, A. I. *J. Phys. Chem. A* **2006**, *110*, 13667.
(27) Burshtein, A. I.; Yakobson, B. I. *Chem. Phys.* **1978**, *28*, 415.
(28) Doktorov, A. B.; Lukzen, N. N. *Chem. Phys. Lett.* **1981**, *79*, 498.
(29) Burshtein, A. I.; Khudyakov, I. V.; Yakobson, B. I. *Prog. React. Kinet.* **1984**, *13*, 221–305.
(30) Temkin, S. I.; Yakobson, B. I. *J. Phys. Chem.* **1984**, *88*, 2679.

JP809015T